Journal of Experimental Botany, Vol. 71, No. 3 pp. 1039–1052, 2020
doi:10.1093/jxb/erz495 Advance Access Publication November 2, 2019

RESEARCH PAPER

Sugar sensing responses to low and high light in leaves of the C_4 model grass *Setaria viridis*

Clémence Henry[1,*], Alexander Watson-Lazowski[1], Maria Oszvald[2], Cara Griffiths[2], Matthew J. Paul[2], Robert T. Furbank[3] and Oula Ghannoum[1]

[1] ARC Centre of Excellence for Translational Photosynthesis, Hawkesbury Institute for the Environment, Western Sydney University, Locked Bag 1797, Penrith NSW 2751, Australia
[2] Plant Science, Rothamsted Research, West Common, Harpenden, Hertfordshire AL5 2JQ, UK
[3] ARC Centre of Excellence for Translational Photosynthesis, Research School of Biology, Australian National University, Acton ACT 2601, Australia

* Correspondence: clemence.henry84@gmail.com

Received 21 March 2019; Editorial decision 11 October 2019; Accepted 4 November 2019

Editor: Christine Raines, University of Essex

Abstract

Although sugar regulates photosynthesis, the signalling pathways underlying this process remain elusive, especially for C_4 crops. To address this knowledge gap and identify potential candidate genes, we treated *Setaria viridis* (C_4 model) plants acclimated to medium light intensity (ML, 500 µmol m^{-2} s^{-1}) with low (LL, 50 µmol m^{-2} s^{-1}) or high (HL, 1000 µmol m^{-2} s^{-1}) light for 4 d and observed the consequences on carbon metabolism and the transcriptome of source leaves. LL impaired photosynthesis and reduced leaf content of signalling sugars (glucose, sucrose, and trehalose-6-phosphate). In contrast, HL strongly induced sugar accumulation without repressing photosynthesis. LL more profoundly impacted the leaf transcriptome, including photosynthetic genes. LL and HL contrastingly altered the expression of hexokinase (HXK) and sucrose-non-fermenting 1 (Snf1)-related protein kinase 1 (SnRK1) sugar sensors and trehalose pathway genes. The expression of key target genes of HXK and SnRK1 were affected by LL and sugar depletion, while surprisingly HL and strong sugar accumulation only slightly repressed the SnRK1 signalling pathway. In conclusion, we demonstrate that LL profoundly impacted photosynthesis and the transcriptome of *S. viridis* source leaves, while HL altered sugar levels more than LL. We also present the first evidence that sugar signalling pathways in C_4 source leaves may respond to light intensity and sugar accumulation differently from C_3 source leaves.

Keywords: C_4 photosynthesis, glucose, hexokinase (HXK), *Setaria viridis*, sucrose, sucrose-non fermenting 1 (Snf1)-related protein kinase 1 (SnRK1); sugar signalling, target of rapamycin (TOR), trehalose-6-phosphate.

Introduction

Plant growth depends on sugar production in source leaves and sugar utilization by sink tissues (e.g. grains, roots, and young leaves). Photosynthesis and sink demand are tightly coordinated through metabolic and signalling feedback regulation. Sugar signalling integrates sugar production with plant development and environmental cues (Rolland *et al.*, 2006). In C_3 plants,

Abbreviations: A_{net}, net photosynthetic rate; CCM, CO_2-concentrating mechanism; C_i, internal CO_2 concentration; DE, differentially expressed; FC, fold change; F_o, minimal fluorescence signal (zero subtracted), dark adapted; F_o', minimal fluorescence signal (zero subtracted), light adapted; F_m', maximum fluorescence signal (zero subtracted), light adapted; F_s, steady-state fluorescence; g_s, stomatal conductance; HL, high light; HXK, hexokinase; LL, low light; ML, medium light; NADP-ME, NADP-malic enzyme; PEPC, phosphoenolpyruvate carboxylase; S6P, sucrose-6-phosphate; SnRK1, sucrose-non-fermenting 1 (Snf1)-related protein kinase 1; T6P, trehalose-6-phosphate; TOR, target of rapamycin; TPP, trehalose-6-phosphate phosphatase; TPS, trehalose-6-phosphate synthase; TRE, trehalase.

sugar accumulation in source leaves, due to source–sink imbalance, negatively feedbacks on photosynthesis and plant productivity (Goldschmidt and Huber, 1992; Krapp and Stitt, 1995; Paul and Foyer, 2001; Paul and Pellny, 2003). However, we have a lack of understanding regarding the molecular mechanisms underlying such feedback regulations, especially in C_4 plants. Addressing this research gap is critical because improving crop yield requires a better understanding of how plants coordinate source activity with sink demand.

C_4 photosynthesis evolved from the ancestral C_3 pathway ~30 million years ago following a drop in atmospheric CO_2 which limited the productivity of C_3 plants in warm climates (Sage *et al.*, 2012). During C_4 photosynthesis, CO_2 is concentrated around Rubisco, the rate-limiting enzyme of the Calvin (C_3) cycle through a CO_2-concentrating mechanism (CCM) to enhance the productivity and efficiency of C_4 plants (Hatch, 1987; Ghannoum *et al.*, 2011). About 50% of C_4 plants are grasses which include some of the world's major staple food, fodder, and biofuel crops, such as maize, sugarcane, sorghum, millets, *Miscanthus*, and switchgrass.

Hexokinase (HXK) was the first sugar sensor identified in plants (Jang and Sheen, 1994; Jang *et al.*, 1997) and is well known for its feedback regulation of photosynthesis and yield through its glucose signalling function. In maize mesophyll protoplasts, the activity of the promoter of seven photosynthetic genes was strongly repressed (3- to 20-fold) by high concentrations (300 mM) of glucose or sucrose (Sheen, 1990). Using sugar analogues, mutants, and transgenic approaches, *AtHXK1* was shown to trigger the glucose repression of photosynthetic rates, stomatal conductance, expression of photosynthetic genes, plant growth, and yield (Jang *et al.*, 1997; Dai *et al.*, 1999; Xiao *et al.*, 2000; Moore *et al.*, 2003; Kelly *et al.*, 2012, 2013, 2014; Brauner *et al.*, 2015). Rice *OsHXK5* and *OsHXK6* were found to have a similar function to *AtHXK1*, showing that this pathway is conserved among plant species (Cho *et al.*, 2008). The role of HXK is yet to be confirmed in intact leaves of C_4 plants under physiological conditions.

The target of rapamycin (TOR) complex is another glucose sensor. TOR promotes plant development and growth under favourable environmental conditions (Dobrenel *et al.*, 2011; Henriques *et al.*, 2014; Rexin *et al.*, 2015; Xiong and Sheen, 2015). Studies using TOR-specific inhibitors, mutants, and transgenic plants showed that the TOR complex is involved in the glucose-dependent induction of photosynthesis, water use efficiency, chlorophyll metabolism, photosynthetic gene expression, stress tolerance, growth, and yield (Xiong *et al.*, 2013; Dong *et al.*, 2015; L. Li *et al.*, 2015; Bakshi *et al.*, 2017; Xiong *et al.*, 2017). However, a clear link between TOR and photosynthesis or growth of C_4 plants is yet to be established.

The sucrose-non-fermenting 1 (Snf1)-related protein kinase 1 (SnRK1) complex is a starvation sensor, generally involved in stress response and survival, and usually acts antagonistically to the TOR complex (Tomé *et al.*, 2014; Li and Sheen, 2016; Baena-González and Hanson, 2017). The SnRK1 complex is directly inhibited by trehalose-6-phosphate (T6P), a sensing sugar which is a proxy for sucrose levels. SnRK1 becomes active under unfavourable environmental conditions to suppress growth and promote survival (Zhang *et al.*, 2009; Tomé *et al.*, 2014; Figueroa and Lunn, 2016; Griffiths *et al.*, 2016). Photosynthesis gene expression is activated by SnRK1 overexpression (Baena-Gonzalez *et al.*, 2007); however, there is limited evidence for a direct link between the SnRK1 complex activity and photosynthesis (Cho *et al.*, 2012; Nukarinen *et al.*, 2016).

Transgenic modification of the T6P pathway in tobacco showed that increased leaf T6P content enhanced photosynthetic capacity per unit leaf area, whilst reducing leaf area and photosynthesis per plant (Pellny *et al.*, 2004). In maize with genetically impaired T6P accumulation in sink tissues, photosynthetic rates were indirectly increased in source leaves, suggesting that T6P could mediate sink regulation of photosynthesis, perhaps through interaction with SnRK1 (Oszvald *et al.*, 2018). In maize source leaves, salt stress reduced photosynthesis whilst increasing sugar concentation (sucrose, glucose, and T6P only at the silking stage), which resulted in the repression of SnRK1 *in vitro* activity but not in clear changes of key downstream targets of SnRK1 (Henry *et al.*, 2015).

The great majority of studies of the role of sugar signalling in photosynthesis have been conducted on C_3 plants such as Arabidopsis, tomato, tobacco, bean, wheat, and rice. Only a few studies used C_4 species. In addition, a very limited number of studies have assessed how sugar signalling regulates photosynthesis through physiological or environmental alterations of sugar contents in intact plants (Bläsing *et al.*, 2005), as opposed to artificially feeding sugars. Sugar signalling in C_4 photosynthesis is important not only in the context of C_4 crop improvement, but also for bioengineering more productive C_3 crops with superior photosynthetic C_4 traits. Alongside transferring superior C_4 photosynthetic traits into major C_3 staple crops such as rice (Karki *et al.*, 2013; Wang *et al.*, 2016), we need a better understanding of how source activity and sink demand are coordinated in the complex C_4 mechanism. This includes fundamental differences in sugar signalling mechanisms that may exist between C_3 and C_4 plants, and the way they may impact photosynthesis, plant productivity, and crop yield. The anatomical and biochemical specializations needed to achieve a C_4 photosynthesis add complexities in extending a putative signalling model from C_3 to C_4 plants (Hatch, 1987; Lunn and Furbank, 1997, 1999; Leegood, 2000).

The overall aim of our study was to explore the relationship between photosynthesis and sugar signalling in C_4 plants. As sugar signalling mutants are not available in C_4 plants, we used the C_4 model species *Setaria viridis* (green foxtail millet) to start identifying gene targets. *Setaria viridis* has recently become a genetic model species to study C_4 photosynthesis due to its small size, short life cycle, small sequenced genome, transformability, and very close phylogenetic relationship to all the main C_4 crops belonging to the same NADP-malic enzyme (NADP-ME) subtype (Brutnell *et al.*, 2010; Li and Brutnell, 2011; Pant *et al.*, 2016). Here, we induced endogenous strong and rapid physiological changes in sugar levels and photosynthesis in C_4 source leaves by varying light intensity over 4 d using low (50 μmol m^{-2} s^{-1}) and high (1000 μmol m^{-2} s^{-1}) light intensities. We focused on the source leaf to directly explore the relationship between sugar signalling and photosynthesis.

Materials and methods

Plant material, growth conditions, and sampling

Wild-type *Setaria viridis* A10 seeds (stock from Hugo Alonso Cantabrana, ANU, Canberra, Australia) were treated for 24 h at 28 °C with 5% liquid smoke (Hickory, Wright's, USA) to release dormancy (Sebastian *et al.*, 2014). Several seeds were planted ~2 cm below ground in 0.3 litre (9 cm top/7.5 cm base×10 cm height) black plastic pots (Reko, Australia) filled with 'Osmocote seed raising and cutting mix' (Scotts, Australia), sprayed with water from the top (regularly for the first few days only to ensure good germination), and placed in trays filled halfway with nutrient solution (0.8 g l^{-1} of Thrive all-purpose soluble fertilizer, Yates, Australia). Plants were grown for 3 weeks in three separate reach-in growth cabinets (GC-20-BDAF model, BioChambers, Canada) under the following conditions: 500 µmol m^{-2} s^{-1} (measured at canopy level) of light provided by a mix of 6400 W high-pressure sodium lamps and 6400 W metal halide lamps; 16 h day:8 h night, 28 °C day:22 °C night; 400 ppm CO_2, and 60% relative humidity (control conditions). To ensure full homogeneity between the chambers, plants were rotated weekly between and within the chambers for the first 3 weeks. Two weeks after planting, fungicide treatment (5 g l^{-1} Mancozeb plus, Yates) was gently sprayed on the canopy to prevent pathogenic infection. Three weeks after planting, treatments started by changing the light intensity in the chambers to low light (LL; 50 µmol m^{-2} s^{-1}), medium light (ML; 500 µmol m^{-2} s^{-1}), or high light (HL; 1000 µmol m^{-2} s^{-1}), respectively, with the same photoperiod, temperature, and relative humidity as before, for four consecutive days. Measurements and sampling were made from day 0 (before treatment) to day 4.

Photosynthetic measurements

Leaf photosynthesis, internal CO_2 concentration, and stomatal conductance were determined using the LI-6400XT open gas exchange system coupled to the 6400-40 leaf chamber fluorometer (Licor, Lincoln, NE, USA). For each treatment and time point, measurements were taken on the mid-section of the last fully expanded leaf on the main shoot of 4–5 independent plants. Measurements were carried out between 9 am and 4 pm (1–8 h after lights were turned on). Gas exchange instruments were randomized between plants, treatments, and days. Leaf area was measured using engineering paper before clamping the leaf in the chamber.

Maximal leaf photosynthetic capacity and fluorescence (F_o, F_s, F_m', and F_o') were measured at high light intensity of 1000 µmol m^{-2} s^{-1} (with 10% blue), reference CO_2 concentration of 400 ppm, leaf temperature of 28 °C, and relative humidity of ~50–60%. Measurements were auto-logged every minute for 45–150 min depending on the treatment, with infrared gas analysers (IRGAs) matched every 2 min. Once leaves reached a steady state, maximum photosynthesis and fluorescence were measured. Plants exposed to LL took progressively longer to reach steady state. Subsequently, A_{net}/C_i response curves were measured by gradually changing CO_2 concentration in the leaf chamber as follows: 50, 100, 150, 200, 300, 400, 600, 800, 1200, 1800, and 400 ppm.

Photosynthesis and fluorescence were also measured at growth light intensity of 500 (day 0) and 50 (LL), 500 (ML), or 1000 (HL) µmol m^{-2} s^{-1} (days 1–4) depending on the treatments. Other conditions were kept the same as described above.

Photosynthetic enzymes in vitro assays, western blots, and chlorophyll content determination

Samples were collected in the light and leaf area was measured before they were snap-frozen in liquid N_2 and stored at −80 °C. To measure phosphoenolpyruvate carboxylase (PEPC), NADP-ME, and Rubisco activity, we used a method adapted from (Sharwood *et al.*, 2016*b*). Briefly, leaf soluble proteins were extracted in an N_2-sparged extraction buffer [50 mM EPPS-NaOH pH 7.8, 5 mM $MgCl_2$, 1 mM EDTA, 5 mM DTT, 1% (w/v) polyvinylpolypyrrolidone (PVPP) and 1% (v/v) plant protease inhibitor cocktail (PIC; Sigma-Aldrich)] from frozen samples. Soluble proteins (10 µl) were then added to a reaction mix to 485 µl of PEPC (50 mM EPPS-NaOH pH 8, 0.5 mM EDTA, 0.2 mM NADH, 5 mM glucose-6-phosphate, 1 mM $NaHCO_3$, 0.5 U of malate dehydrogenase, and 10 mM $MgCl_2$), NADP-ME (49.25 mM Tricine-KOH pH 8.3, 4 mM $MgCl_2$, 0.5 mM NADP, and 0.1 mM EDTA), or Rubisco (50 mM EPPS-NaOH pH 8, 0.5 mM EDTA, 0.2 mM NADH, 1 mM ATP, 5 mM creatine phosphate, 20 mM $NaHCO_3$, 10 µl of coupling enzymes, and 10 mM $MgCl_2$) reaction buffers incubated at 25 °C. PEPC, NADP-ME, and Rubisco reactions were then started by adding 5 µl of PEP (4 mM final), malate (5 mM final), or RuBP (0.22 mM final), respectively. The NAD^+/H reduction or oxidation were then monitored at 340 nm and the initial slopes were used to calculate the enzyme activities (Sharwood *et al.*, 2014, 2016*a*) (Supplementary Protocol S1 at *JXB* online). In addition, 300 µl of the fresh soluble fraction extracted for the assay was mixed with 100 µl of NuPAGE LDS Sample Buffer (4×) (Life Technologies), snap-frozen in liquid N_2, and stored at −80 °C for SDS–PAGE and western blot analysis. SDS–PAGE and immunoblot analysis of photosynthetic proteins (PEPC, NADP-ME, and Rubisco) were carried out as in (Sharwood *et al.*, 2014) (Supplementary Protocol S2).

Protein content in the soluble extract was determined by using the Pierce™ Coomassie Plus (Bradford) Assay Reagent (Thermo Scientific), BSA as a standard, 96-well plates, and the CLARIOstar Microplate Reader (BMG LabTech Pty Ltd). Chlorophyll content was determined using 100 µl of crude extract from the tissue lysate used for the enzymatic assays and western blots according to the acetone extraction and quantification method described by Porra *et al.* (1989).

Analysis of metabolites and in vitro SnRK1 activity

Measurements of glucose, fructose, sucrose, sucrose-6-phosphate (S6P), trehalose-6-phosphate (T6P), and trehalose were performed by Metabolomic Discoveries (Germany) using the method described by Kretzschmar *et al.* (2015). Briefly, metabolites were extracted from frozen leaf tissues and analysed by LC-MS. Measurements were then compared with samples from ML day 0 plants (control) and adjusted for fresh weight. Measurements were performed on four independent biological replicates for each treatment and time point.

SnRK1 *in vitro* activity was determined using a method adapted from Zhang *et al.* (2009). A 150–300 mg aliquot of frozen leaf samples was ground in liquid N_2 and homogeneized in ice-cold extraction buffer [100 mM Tricine-NaOH pH 8.2, 25 mM sodium fluoride, 0.5 mM EGTA, 0.5 mM EDTA, 1 mM benzamidine, 5 mM DTT, 20% (w/v) PVPP, 1× PIC (P9599, Sigma-Aldrich), and 0.5× general non-specific phosphatase inhibitor cocktail (500 mM sodium fluoride, 250 mM β-glycerophosphate, 100 mM sodium pyrophosphate, 20 mM sodium orthovanadate)]. After centrifugation, soluble protein extracts were desalted through an NAP-10 column (GE Healthcare, UK) pre-equilibrated with resuspension buffer (100 mM Tricine-NaOH pH 8.2, 25 mM sodium fluoride, 0.5 mM EGTA, 0.5 mM EDTA, 1 mM benzamidine, 5 mM DTT) and resuspended in 1.5 ml of resuspension buffer added with 1× PIC and 1 µM okadaic acid. Soluble protein extracts were then aliquoted, snap-frozen in liquid N_2, and stored at −80 °C until used for the assays. SnRK1 activities were determined in a final volume of 25 µl in microtiter plate wells at 30 °C. Assay medium contained 40 mM HEPES-NaOH pH 7.5, 5 mM $MgCl_2$, 4 mM DTT, 0.5 µM okadaic acid, 1× PIC, 200 µM ATP containing 12.5 kBq of [γ-^{33}P]ATP (PerkinElmer), added with or without (negative control) 200 mM of AMARA peptide (Enzo Life Science). For T6P inhibition assays, a final concentration of 1 mM T6P (T4272, Sigma-Aldrich) was added to the mix. Assays were started with the addition of 5 µl of protein extract and stopped after 4 min by transferring 15 µl of reaction mix to a 2 cm^2 Protran 0.45 µm nitrocellulose membrane (GE) immediately immersed in ultra-purified water. Membranes were then washed four times with 800 ml of ultra-purified water, air-dried, and transferred to 5 ml scintillation vials with 3.5 ml of scintillation cocktail (Ultima Gold). Radioactivity was then determined using a scintillation counter. For each time point, the assays were performed on four independent biological replicates in duplicate or triplicate.

Next-generation RNA sequencing and functional gene annotation

Total RNA was extracted from ~10 mg of finely ground frozen source leaf samples (collected at the same time as samples used for the enzyme assays above) using Purezol (Biorad), resuspended in 50 µl of RNA secure resuspension solution (Ambion), and stored at −80 °C. Aliquots of RNA from each sample were then treated with DNase I (Ambion) following the manufacturer's protocols, before library preparation using a TruSeq Stranded RNA HT Kit for Plants (Illumina) was carried out. RNA sequencing was then performed using an Illumina Hi-Seq 2500 machine with 125 bp paired-end sequencing by the Western Syndey University Next Generation Sequencing facility. Between 17 and 25 million reads were returned per sample. Raw reads can be found in GenBank under BioProject accession number PRJNA493674. Raw reads were pre-processed using Trimmomatic (Bolger *et al.*, 2014) to trim adaptors. Transcript expression was calculated via mapping the processed reads to the closely related *S. italica* transcriptome (v2.2) (Bennetzen *et al.*, 2012) using DEW (http://dew.sourceforge.net/), an automated pipeline which utilizes Bowtie2 (Langmead and Salzberg, 2012) to align reads against a given reference, then eXpress (Roberts and Pachter, 2013) to calculate normalized transcript expression (transcripts per million; TPM). Differentially expressed (DE) transcripts were identified using DEApp (Li and Andrade, 2017) utilizing DESeq2 (Love *et al.*, 2014). A minimum read count of 1 count per million (CPM) in at least two replicates and a false discovery rate (FDR) cut-off of ≤0.05 were used to identify DE transcripts. In order to not be overly stringent, we chose not to apply a minimum threshold in terms of fold change (FC), but instead to classify all DE transcripts into three groups: slightly (<2 FC), mildly (between 2 and 5 FC), and highly (>5 FC) DE transcripts. Heat maps were then generated using these groups. The exact FC of each DE transcript and the group to which they belong can be found in Supplementary Table S5.

Predicted protein sequences are readily available for the *S. italica* genome v2.2 (Foxtail millet, https://phytozome.jgi.doe.gov/pz/portal.html) (Bennetzen *et al.*, 2012) and so were used to annotate all transcripts identified in our experiments. In addition to the pre-existing annotations of *S. italica* proteins, we used Mercator4 (beta version, http://plabipd.de/portal/web/guest/mercator-ii-alpha-version-) (Lohse *et al.*, 2014) in order to obtain the Mapman 4 (Thimm *et al.*, 2004) annotation for each protein. Additional *S. italica* transcripts were also annotated as C_4 photosynthetic genes, sugar sensors, trehalose pathway genes, and putative sugar signalling targets (Supplementary Tables S6–S12), and were determined using published RNA sequencing (RNA-Seq) and microarray data from both Arabidopsis and C_4 grasses (Jang and Sheen, 1994; Jang *et al.*, 1997; Zhou *et al.*, 1998; Sheen *et al.*, 1999; Xiao *et al.*, 2000; Krishna and Gloor, 2001; Sung *et al.*, 2001; Moore *et al.*, 2003; Baena-Gonzalez *et al.*, 2007; Nishimura *et al.*, 2008; Andrès *et al.*, 2010; Caldana *et al.*, 2013; Flores-Pérez and Jarvis, 2013; Kikuchi *et al.*, 2013; Nunes *et al.*, 2013; Xiong *et al.*, 2013; John *et al.*, 2014; Kunz *et al.*, 2014, 2015; Nakai, 2015; Trösch *et al.*, 2015; Sharwood *et al.*, 2016*a*; Bracher *et al.*, 2017; Watson-Lazowski *et al.*, 2018) (studies used are detailed in Supplementary Protocol S3). For the sugar sensing targets, only those that behaved consistently within multiple studies were selected and annotated as such.

Statistical analysis

To assess significant changes in morphological, physiological and biochemical results, we performed a two-way ANOVA followed by an *F*-test using R (R Core Team, 2016) and RStudio (RStudio Team, 2015) to assess the effect of both treatment and time, as well as their interaction on each of the tested parameters. We also ensured that the distribution of the ANOVA was 'normal' using a quantile–quantile plot (qqPlot). To assess the effect of LL and HL treatments compared with the ML control for each time point, we performed a one-way ANOVA followed by a Tukey test. For each parameter tested, we indicated significant differences ($P<0.05$) between the treatments and the control with an asterisk.

Results

To quickly and strongly alter *in vivo* sugar levels and trigger related changes in sugar signalling and photosynthesis in C_4 leaves, we treated 3-week-old *S. viridis* plants acclimated to ML intensity (500 µmol m^{-2} s^{-1}, control) with low or high light intensity (LL=50 µmol m^{-2} s^{-1} or HL=1000 µmol m^{-2} s^{-1}, respectively) (Supplementary Fig. S1A). Based on our preliminary experiments, 4 d of treatment were required and sufficient to trigger significant changes in sugar levels and photosynthetic capacity (Figs 1, 2), validating the experimental system used here.

LL strongly impaired photosynthesis of S. viridis*, while HL had little effect*

By day 4, LL-treated plants had reduced growth and turgor, while HL-treated plants showed the opposite effect when compared with control (ML) plants (Supplementary Fig. S1B). In control and HL-treated *S. viridis*, leaves typically took 25 min to reach steady-state photosynthesis (A_{net}) measured at high irradiance (1000 µmol m^{-2} s^{-1}) (Supplementary Fig. S2). From day 1, LL strongly delayed (up to 150 min) the time for leaves to reach steady-state A_{net} at high irradiance (Supplementary Fig. S2). After 25 min of equilibration, LL reduced A_{net} (–65%) and stomatal conductance (g_s; –55%), and increased internal CO_2 concentration, C_i (+75%), starting from day 2 when compared with the control (Fig. 1A–C). When leaves were allowed to fully adjust to high irradiance, LL significantly reduced steady-state A_{net} (–27%) and g_s (–19%), and increased C_i (+36%) on day 4 only (Fig. 1D–F), indicating the onset of photosynthetic impairment. Reduced photosynthetic capacity on day 4 under LL, following full acclimation to high irradiance (Fig. 1D–F), was correlated with significant reductions in the initial slope (–49%) and maximum rate (–26%) of the A–C_i curves relative to the control (Supplementary Table S1; Supplementary Fig. S3), as well as fluorescence parameters (F_v'/F_m' and electron transport rate) (Supplementary Table S1). In contrast, HL had no effect on any of the photosynthetic parameters (Supplementary Fig. 1; Fig. S3; Supplementary Table S1).

When measured at growth irradiance, photosynthesis and electron transport rates were near zero in LL plants, which also had higher maximum efficiency of PSII (F_v'/F_m') and photochemical quenching (qP) relative to the control. HL plants had slightly higher photosynthesis and electron transport rates when measured at growth light, but lower F_v'/F_m' and qP relative to control plants (Fig. 1G–I; Supplementary Table S1).

LL induced a gradual decrease (approximately –50%) in the activity and content of PEPC (day 2) and NADP-ME (day 3), and the activation state of Rubisco (day 1) relative to control plants. HL increased the *in vitro* activity and content of PEPC (significantly by day 3) but had no significant effect on NADP-ME or Rubisco relative to the control (Supplementary Fig. S4). Chlorophyll content was unaffected by the light treatment, and hence cannot explain the observed photosynthetic changes (Supplementary Table S1).

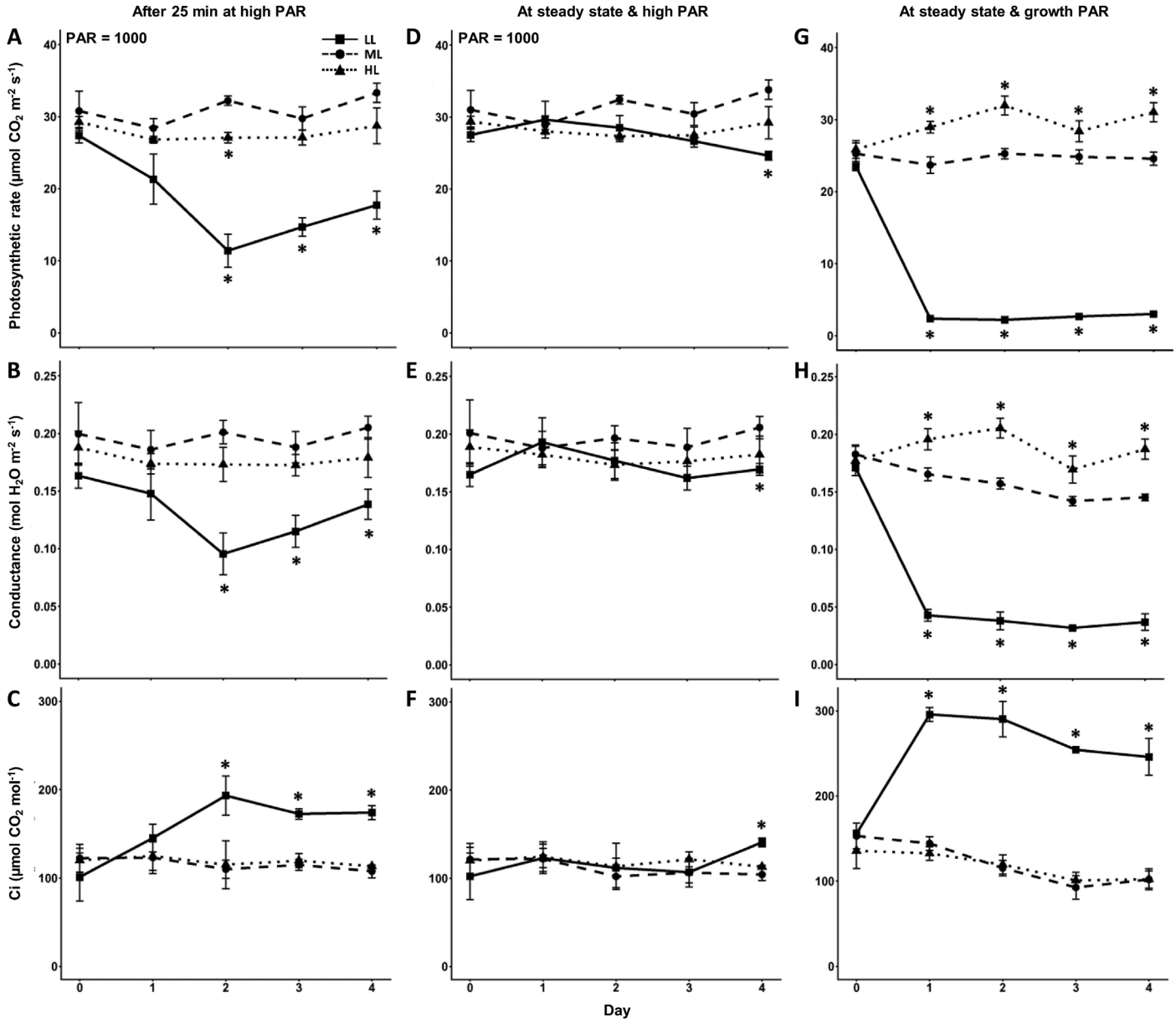

Fig. 1. Photosynthetic capacity of *S. viridis* plants is strongly impaired by low light while it is not affected by high light. Dynamic changes in photosynthetic rates (A, D, and G), leaf conductance (B, E, and H), and leaf internal CO_2 concentration (C, F, and I) of low light (LL; 50 μmol m^{-2} s^{-1}), medium light (ML; 500 μmol m^{-2} s^{-1}, control), and high light (HL; 1000 μmol m^{-2} s^{-1}) treated *S. viridis* plants provided with high light intensity (1000 μmol m^{-2} s^{-1}, 10% blue light) or growth light intensity (50, 500, or 1000 μmol m^{-2} s^{-1}, 10% blue light) and current ambient CO_2 reference concentration (400 ppm) for gas exchange measurements. For every time point, the midsection of the last fully expanded leaf was clamped to the gas exchange chamber and measurements were taken every minute for up to 1.5 h after clamping. Here we present measurements taken 25 min after clamping (A–C) as well as when plants reached their maximum photosynthetic rates at steady state (D–I). All measurements were carried out from morning to early afternoon on 3–5 different plants for each time point and treatment. Asterisks indicate statistical differences (P<0.05) between the treated and control plants for each given time point

HL had a greater impact than LL on the content of signalling sugars

LL gradually reduced the relative content of key sugars involved in sugar signalling (glucose, sucrose, and T6P) as well as other key sugars (fructose, S6P, and trehalose), while HL caused a strong gradual increase in sugar accumulation relative to the control (Fig. 2: Supplementary Fig. S5). The relationship between photosynthesis measured at growth light and sugar content was exponential; photosynthesis and sugars increased abruptly from LL to ML, then photosynthesis plateaued with further sugar increases between ML and HL (data not shown).

SnRK1 starvation sensor was indirectly modulated by changes in T6P content, but not directly by the light treatment

The *in vitro* kinase (total or T6P inhibited) activities of SnRK1 were generally unaffected by the light treatment over the course of the experiment. Addition of T6P (1 mM) to the reaction mix reduced the SnRK1 *in vitro* kinase activity to 30–65% of the total activity in all samples (Fig. 3). No correlation was found between photosynthetic rates at growth light and the total or T6P-inhibited activity of SnRK1 (data not shown). However, *in vivo* changes in T6P content under

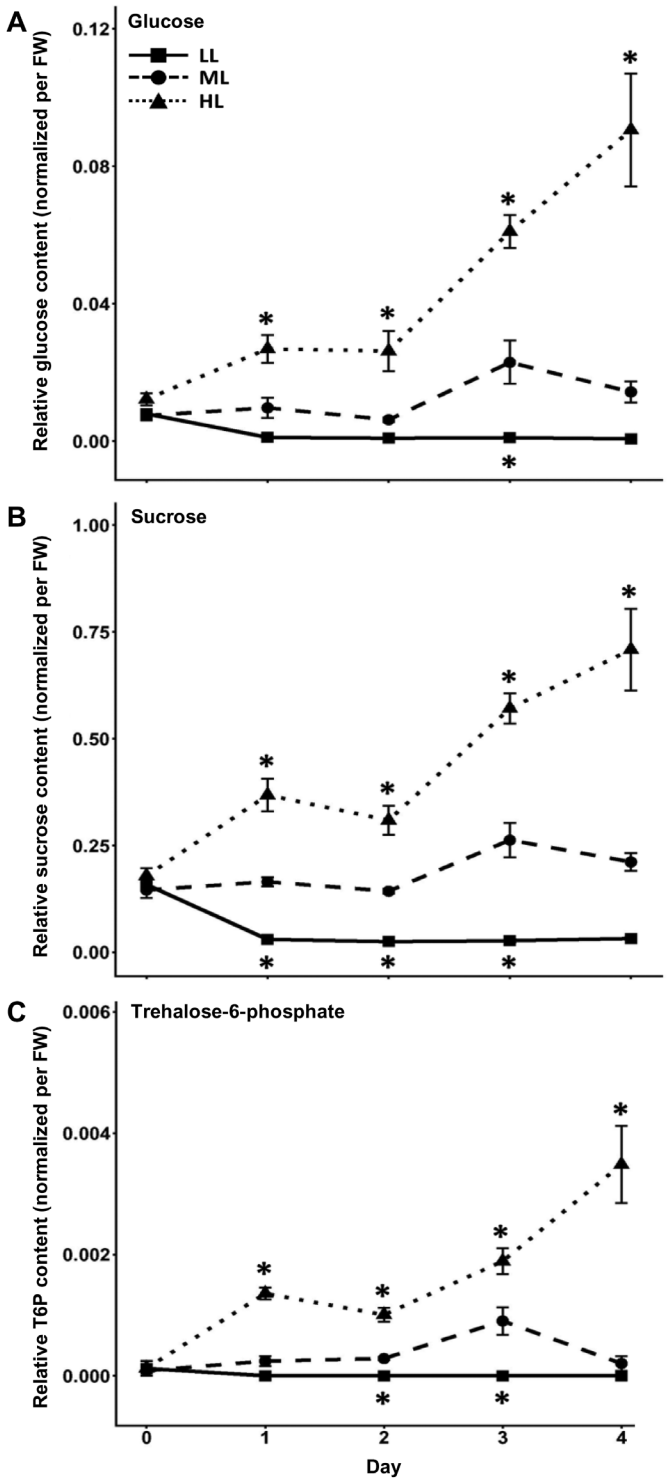

Fig. 2. Low light gradually reduces the levels of key sugars in the leaves of *S. viridis* while high light causes a strong and gradual build up of those sugars over time. Dynamic changes in glucose (A), sucrose (B), and trehalose-6-phosphate (C) content in fully expanded leaves of LL (50 µmol m^{-2} s^{-1}), ML (500 µmol m^{-2} s^{-1}), and HL (1000 µmol m^{-2} s^{-1}) treated *S. viridis* plants before and during treatment. Sugars were extracted from leaf blade samples collected from the midsection of the last fully expanded leaf at midday (6 h after lights were turned on). Sugar levels were measured using semi-quantitative LC-MS. Sugar levels are semi-quantitative, expressed relative to day 0 ML samples and normalized per fresh weight. For each treatment and time point, the assays were carried out on four independent biological replicates. Asterisks indicate statistical differences (P<0.05) between the treated and control plants for each given time point

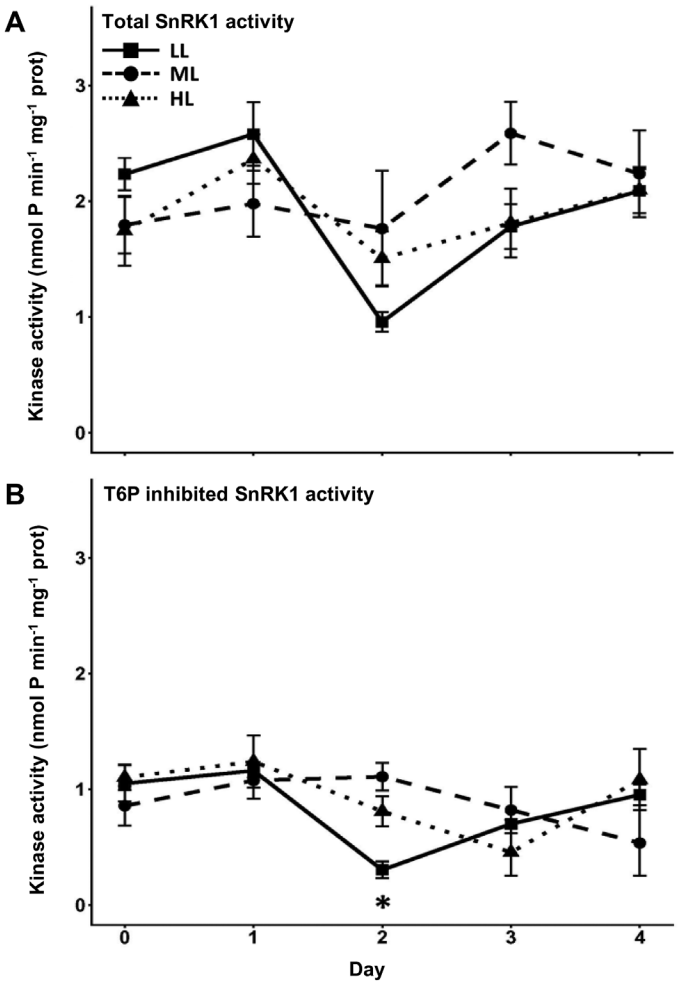

Fig. 3. SnRK1 *in vitro* activity of *S. viridis* leaves is not significantly affected by low or high light treatment, but is reduced to about half in the presence of T6P. Dynamic changes in total (A) and T6P inhibited (B) SnRK1 *in vitro* kinase activity from protein extracts of fully expanded *S. viridis* leaves treated with LL (50 µmol m^{-2} s^{-1}), ML (500 µmol m^{-2} s^{-1}), and HL (1000 µmol m^{-2} s^{-1}). For SnRK1 inhibition assays (B), 1 mM of exogenous T6P was added to the reaction. Kinase activities were normalized per amount of total proteins. For each treatment and time point, the assays were carried out on four independent biological replicates. Asterisks indicate statistical differences (P<0.05) between the treated and control plants for each given time point

LL and HL were associated with altered expression of key SnRK1 downstream targets, favouring activation and repression of SnRK1 under LL and HL, respectively (Figs 2, 6). These results suggest that SnRK1 activity in *S. viridis* leaves was modulated through changes in T6P contents rather than through a direct modulation of the kinase activity by light in our experimental system.

LL induced major transcriptomic changes, especially for photosynthetic genes, while HL had little impact

On day 0, only 0–3 genes were differentially expressed between the treated plants and the controls, demonstrating that observed responses on subsequent days were caused by the light treatments and not due to random variations between replicates. At the whole-transcriptome level, 7905 out of 17 459 transcripts

(45%) were significantly differentially expressed at LL and/or HL relative to control (Supplementary Fig. S6; Supplementary Table S2). LL significantly changed the expression of 4608, 3398, and 4373 transcripts on day 1, 2, and 4, respectively. In contrast, HL had limited to no effect on gene expression, with most of the changes occurring on day 1 (1426 DE transcripts) and very few changes observed on day 2 and 4 (191 and 69 DE transcripts, respectively) (Supplementary Table S2).

LL (especially on days 2 and 4) down-regulated the expression of genes involved in photosynthesis, cellular respiration, metabolism of carbohydrates, amino acids, lipids, nucleotides, coenzymes, secondary and reactive oxygen, protein biosynthesis, cell wall, solute transport, and nutrient uptake (Supplementary Table S3). LL up-regulated genes involved in chromatin assembly and remodelling, cell cycle, RNA biosynthesis, and membrane trafficking. Genes involved in protein degradation, phytohormones, cytoskeleton, protein translocation, and DNA damage response were down- or up-regulated in equal numbers by LL. These changes are consistent with a general switch from anabolism to catabolism under a low energy status and limited growth (Supplementary Fig. S1).

On day 1, HL down-regulated the expression of genes involved in RNA biosynthesis, protein degradation, solute transport, phytohormones, and nutrient uptake, and up-regulated the expression of genes involved in protein biosynthesis and translocation, RNA processing, cellular division, carbohydrate, amino acid, and nucleotide metabolism, chromatin assembly and remodelling, cell cycle, and membrane vesicle trafficking (Supplementary Table S3). Some genes involved in protein modification, environmental stimuli response, cell wall, cytoskeleton, coenzyme metabolism, and reactive oxygen metabolism and photosynthesis were down- or up-regulated in equal numbers by HL. These changes are generally consistent with increased anabolism leading to increased growth (Supplementary Fig. S1).

Out of the 301 photosynthetic genes identified, LL down- and up-regulated 74% and 4% of those genes, respectively; while HL down- and up-regulated 2% and 4% of these genes, respectively (Fig. 4; Supplementary Table S2). This demonstrates the profound inhibitory effect of LL on photosynthesis, which led to the observed sugar depletion, as opposed to the minor effects of HL on photosynthesis which were associated with a large amount of sugar accumulation in *S. viridis*.

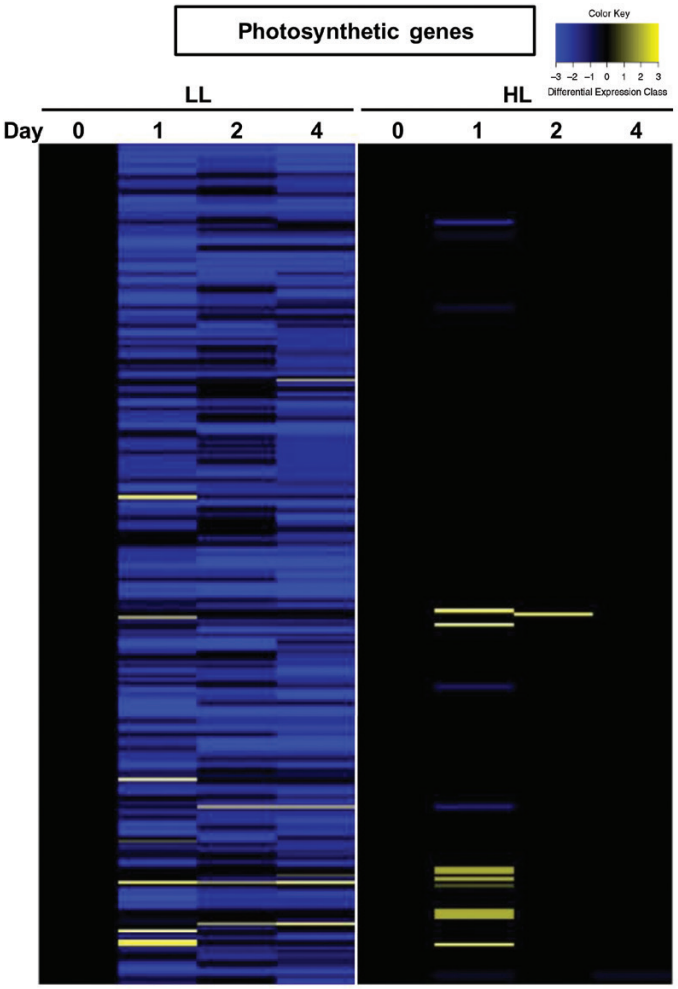

Fig. 4. Low light down-regulates >70% of the photosynthetic gene transcripts expressed in *S. viridis* leaves, while high light has little to no effect on most of them. Heatmap representing the dynamic changes in transcript levels of photosynthetic genes in *S. viridis* leaves treated with LL (50 µmol m^{-2} s^{-1}) and HL (1000 µmol m^{-2} s^{-1}) relative to ML (500 µmol m^{-2} s^{-1}, control) before (day 0) and during treatment (days 1, 2, and 4) using RNA-Seq. A total of 244 out of 301 detected photosynthetic transcripts were differentially expressed between all the conditions. For each treatment, analyses were carried on three independent biological replicates. We used cut-off values of at least 1 CPM in at least two samples and an FDR of 0.05 for the differential expression analysis with DESeq2. Blue and yellow lines, respectively, represent a significant decrease or increase in transcript levels in the treatment compared with the control. Genes were classified based on their respective differential expression as follows (fold change compared with control): (class –3, highly repressed)<–5 FC<(class –2, mildly repressed)<–2 FC<(class –1, slightly repressed)<0 FC=(class 0, unaffected)<(class 1, slightly induced)<2 FC<(class 2, mildly induced)<5 FC<(class 3, highly induced).

LL and HL contrastingly altered the expression of key sugar signalling and trehalose pathway genes

Overall, light treatments significantly (FDR ≤0.05) altered the expression of 42% of the 52 sugar signalling genes identified as expressed in *S. viridis* leaves. Once again, LL had a prominent effect on most of these genes, affecting 40% of them, while HL had a smaller and antagonist effect on them, with only 17% of those genes being affected (Fig. 5; Supplementary Table S2).

In terms of the sugar sensors, LL repressed the expression of *SvHXK5* and *6*, the closest homologues of the *HXK* isoforms able to sense glucose in Arabidopsis and rice. LL also induced the expression of several genes encoding key subunits of both the TOR and SnRK1 energy signalling complexes. On the other hand, HL had no effect on HXK or TOR complex genes, while it repressed the expression of two genes involved in the SnRK1 complex (Fig. 5).

In the trehalose pathway, LL strongly repressed the expression of both transcripts encoding the TPSI.1 [trehalose-6-phosphate synthase (TPS) class I) protein, which is responsible for the synthesis of T6P. In addition, LL induced the expression of several *TPSII* (TPS class II), one trehalose-6-phosphate

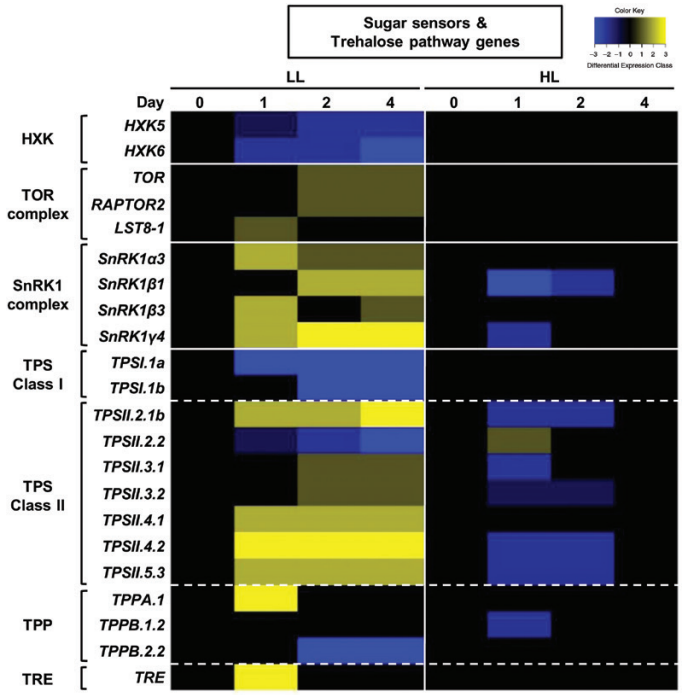

Fig. 5. Low light affects the transcript levels of most of the key sugar sensors and trehalose pathway genes expressed in *S. viridis* leaves, while high light has a smaller but antagonist effect. Heatmap representing the dynamic changes in transcript levels of sugar sensors (HXK, TOR complex, and SnRK1 complex) and the trehalose pathway [trehalose-6-phosphate synthase (TPS), trehalose-6-phosphate phosphatase (TPP), and trehalase (TRE)] genes in leaves treated with LL (50 µmol m^{-2} s^{-1}) and HL (1000 µmol m^{-2} s^{-1}) relative to ML (500 µmol m^{-2} s^{-1}, control) before (day 0) and during treatment (days 1, 2, and 4) using RNA-Seq. A total of 22 out of 52 sugar signalling transcripts were differentially regulated between all the treatments. For each treatment, analyses were carried on three independent biological replicates. We used cut-off values of at least 1 CPM in at least two samples and an FDR of 0.05 for the differential expression analysis with DESeq2. Blue and yellow lines, respectively, represent a significant decrease or increase in transcript levels in the treatment compared with the control. Genes were classified based on their respective differential expression as follows (fold change compared with control): (class –3, highly repressed)<–5 FC<(class –2, mildly repressed)<–2 FC<(class –1, slightly repressed)<0 FC=(class 0, unaffected)<(class 1, slightly induced)<2 FC<(class 2,mildly induced)<5 FC<(class 3, highly induced)

phosphatase (*TPP*), and trehalase (*TRE*) transcripts (Fig. 5), which are respectively potentially responsible for the regulation of TPSI.1, the dephosphorylation of T6P to form trehalose, and the degradation of trehalose into two glucose moieties (Ramon and Rolland, 2007). These changes are consistent with a reduction in T6P biosynthesis and an increase in T6P degradation, which explains the observed reduction in T6P levels under LL (Fig. 2). HL did not alter the expression of *TPSI.1* or *TRE*, but it repressed the expression of most *TPSII* genes which were induced under LL, as well as the expression of *TPPB.1.2* (Fig. 5). These results partly explain the strong increase of T6P levels observed under HL (Fig. 2C). In addition, *AtTPS8–AtTPS10 TPSII* genes are starvation inducible and sugar repressible (Nunes *et al.*, 2013), which is consistent with the respective induction and repression of six and five of the *TPSII* transcripts by LL and HL, respectively in our experiment (Fig. 5).

The expression of key sugar signalling target genes indicated the induction of both the SnRK1- and HXK-dependent signalling pathways by LL, while HL only slightly repressed the SnRK1 pathway

LL clearly altered the expression of well-characterized key downstream targets of both the SnRK1- and HXK-dependent sugar signalling pathways, indicating the activation of both these pathways under LL and sugar depletion in C_4 source leaves, while the TOR signalling pathway was clearly unaffected by LL (Fig. 6; Supplementary Table S2). When considering the full list of putative SnRK1 downstream targets based on protein homology with genes identified in previously published work using C_3 plants, trends were less clear than for the well-characterized targets (Supplementary Fig. S6). The discrepancy may relate to our focus on the source leaf, while most previous studies used Arabidopsis seedlings and sink tissues (e.g. wheat grain, Martínez-Barajas *et al.*, 2011) and/or protoplasts. Using the same list of key HXK, TOR, and SnRK1 downstream targets, HL and sugar accumulation slightly repressed the SnRK1 signalling pathway only, but had no clear effect on either the HXK-dependent or the TOR signalling pathways (Fig. 6). Similar to LL, HL did not have a strong effect on the full list of SnRK1 downstream targets, although it induced a marginal (8–34% of the total transcripts) change in the expression of the putative sugar signalling target genes (Supplementary Fig. S6; Supplementary Table S2). Taken together, our results suggest that, although LL may have induced the SnRK1 signalling pathway through changes in T6P levels in the C_4 source leaves, LL appears to have triggered a different overall sugar signalling response from that previously described in Arabidopsis (C_3). This indicates that the overall set of target genes affected by SnRK1 may differ between organisms (C_3 versus C_4), tissues (sink versus source), and/or development stages (vegetative versus mature stage).

Discussion

Sugar feedback inhibition of C_3 photosynthesis and the role of sugar signalling in controlling sink development have been well studied, but the interplay between sugar signalling and C_4 photosynthesis remains poorly understood. Our study aimed at elucidating this knowledge gap by inducing concurrent changes in photosynthesis and sugar contents at varying light intensity. We hypothesized that C_4 photosynthesis might be less sensitive to sugar feedback inhibition than C_3 photosynthesis due to the fundamental differences between the way these species operate and regulate their sugar metabolism. Our study revealed two key novel findings. First, LL impacted C_4 photosynthesis and the transcriptome of *S. viridis* source leaves more profoundly than HL, even though HL altered sugar levels to a greater extent than LL. Secondly, sugar signalling pathways of C_4 source leaves responded to light intensity and associated sugar accumulation differently from previous reports for C_3 plants using sink tissues, seedlings, or protoplasts. Our results are highly relevant for the improvement of crop yield through a better understanding of the pathways regulating sugar production and allocation in source tissues.

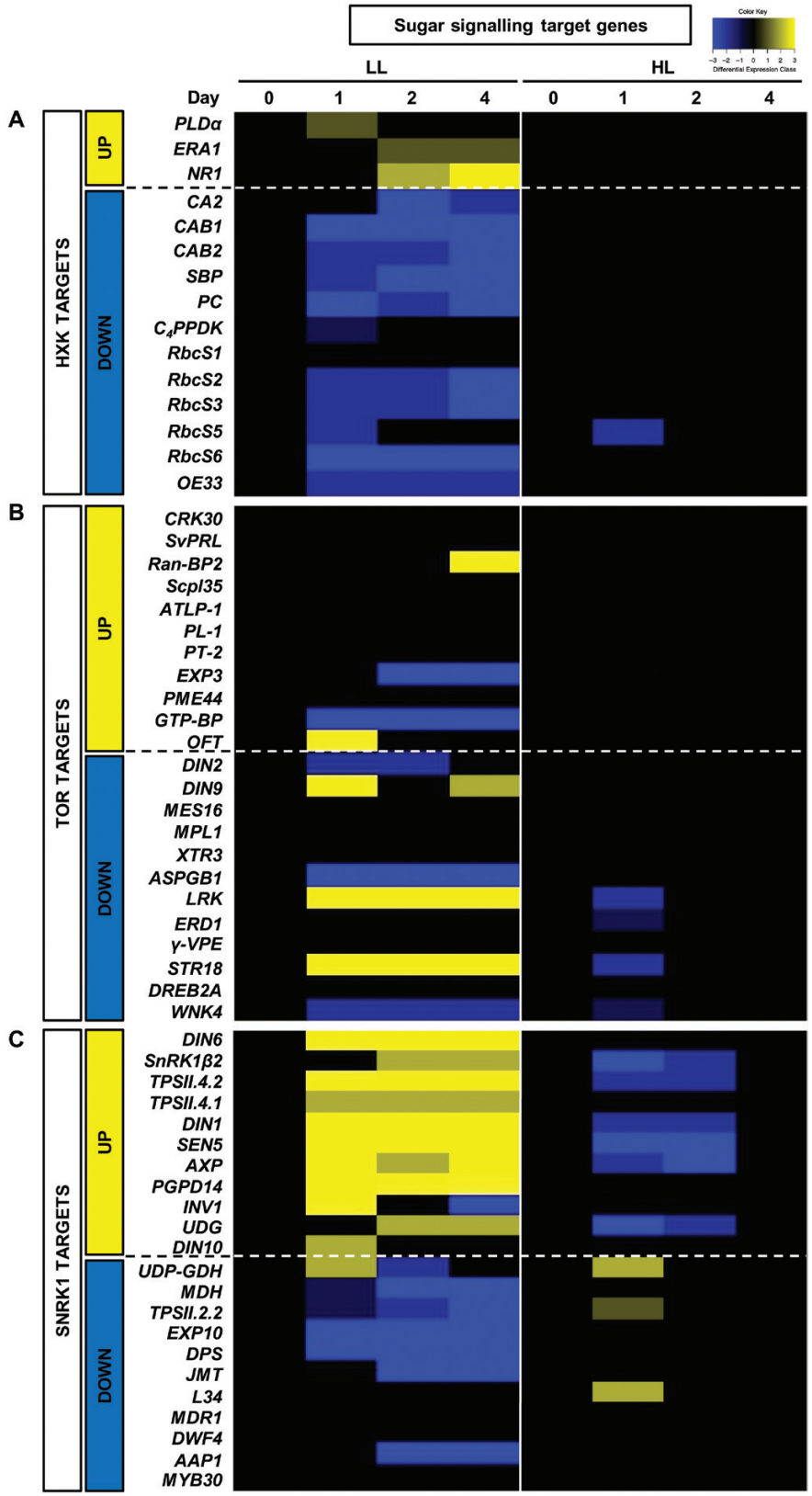

Fig. 6. Light treatment had a clear impact on the expression of key HXK and SnRK downstream targets, but no effect on key TOR downstream targets in mature C_4 *S. viridis* leaves. Heatmaps representing the dynamic changes in transcript levels of key downstream targets of HXK (A), TOR (B), and SnRK1 (C) in mature *S. viridis* leaves treated with LL (50 μmol m^{-2} s^{-1}) and HL (1000 μmol m^{-2} s^{-1}) relative to ML (500 μmol m^{-2} s^{-1}, control) before (day 0) and during treatment (days 1, 2, and 4). For each treatment, analyses were carried on three independent biological replicates. We used cut-off values of at least 1 CPM in at least two samples and an FDR of 0.05 for the differential expression analysis with DESeq2. Blue and yellow lines, respectively, represent a significant decrease or increase in transcript levels in the treatment compared with the control. Genes were classified based on their respective differential expression as follows (fold change compared with control): (class –3, highly repressed)<–5 FC<(class –2, mildly repressed)<–2 FC<(class –1, slightly repressed)<0 FC=(class 0, unaffected)<(class 1, slightly induced)<2 FC<(class 2, mildly induced)<5 FC<(class 3, highly induced).

LL impacted photosynthesis and transcriptome of S. viridis *source leaves more profoundly than HL, while HL altered sugar levels more than LL*

Four days after switching the light intensity, LL profoundly impacted three broad areas: (i) photosynthesis (photosynthetic rates, capacity, enzyme activity and content, and gene expression); (ii) sugar metabolism; and (iii) gene expression of sugar signalling components (HXK, SnRK1, and the trehalose pathway), some of their targets, and the whole transcriptome of C_4 source leaves. In contrast, the main effects of HL were a strong accumulation of sugars without any feedback regulation of photosynthesis and a slight repression of the SnRK1 pathway (Figs 1–6; Supplementary Figs S2, S4; Supplementary Table S2). C_4 species evolved and are adapted to HL (Sage and Pearcy, 2000). In addition, the operation of the CCM and overcycling of CO_2 into the bundle sheath requires additional energy (Hatch, 1987). This partly explains why C_4 plants are generally more sensitive to LL than HL (Usuda and Edwards, 1984; Usuda *et al.*, 1985, 1987; Kalt-Torres *et al.*, 1987).

LL reduced photosynthetic rates of C_4 source leaves to near zero, depleting sugars to very low levels (Figs 1, 2) and reducing plant growth and turgor (Supplementary Fig. S1). Consequently, LL triggered massive and persistent transcriptional changes aimed at promoting cell maintenance and survival (Fig. 6; Supplementary Table S3). In particular, photosynthetic enzymes and 74% of photosynthetic genes were repressed by LL (Fig. 4, Supplementary Fig. S4; Supplementary Table S2). Gene transcription and protein translation are energetically costly processes minimized under energy limitation (Baena-González, 2010; Browning and Bailey-Serres, 2015; Merchante *et al.*, 2017). At the whole-transcriptome level, LL also triggered a general down-regulation of genes involved in anabolism, and an up-regulation of genes involved in catabolism and gene/protein regulation, especially on day 4 (Fig. 6; Supplementary Table S3). These results are consistent with previous work done on C_3 plants, where the transcriptome was strongly affected by prolonged shading (Gong *et al.*, 2014; Ding *et al.*, 2016).

In contrast to LL, HL had little effect on photosynthetic capacity, enzyme activity, or gene expression of *S. viridis* source leaves. Although photosynthetic rates measured at growth light were slightly (+14–26%) increased by HL, HL induced a gradual and strong sugar accumulation (up to 4- to 8-fold on day 4) without inducing any photosynthetic down-regulation (Figs 1, 2). At the whole-transcriptome level, HL altered transcript abundance of three times fewer genes than LL on day 1, and of only very few genes on days 2 or 4 (Supplementary Fig. S6; Supplementary Table S3). On day 1, HL mainly induced transcriptional changes which promoted anabolism without impacting photosynthesis or sugar signalling. Subsequently, HL leaves regained physiological and transcriptional homeostasis while sugars continued to accumulate. Our results contrast with the usual photosynthetic repression associated with the exposure of C_3 leaves to conditions leading to sugar accumulation (Sheen, 1990; Jang and Sheen, 1994; Jang *et al.*, 1997; Dai *et al.*, 1999; Xiao *et al.*, 2000; Kelly *et al.*, 2012).

LL and HL altered sugar levels and elicited unexpected sugar signalling responses in C_4 source leaves that could be due to different sensitivities to sugars, or alternative sugar or light signalling pathways

LL altered the expression of key sugar sensors more than HL (Fig. 5). However, despite the strong changes in glucose and T6P levels under both light treatments (Fig. 2), we did not observe all the expected sugar signalling responses (Fig. 6; Supplementary Table S2). LL altered the transcript abundance of genes encoding HXKs and various components of TOR, SnRK1, and the trehalose pathway. LL also altered the expression of key downstream targets of HXK and SnRK1, indicating that both signalling pathways may be activated under low energy status (Fig. 6). Since most of the downstream targets of HXK are photosynthetic genes, which may also be regulated by light, it was difficult to separate the effects of the sugar- and light-dependent pathways. This point is addressed later in the manuscript.

On the other hand, according to the expression of well-defined sugar sensing target genes, the strong glucose accumulation observed under HL was not associated with the activation of the HXK-dependent or the TOR signalling pathways expected under feast-like conditions (Figs 2, 5, 6). It was especially surprising for the HXK-dependent signalling pathway which typically is associated with the feedback inhibition of photosynthesis (Sheen, 1990). Interestingly, the SnRK1 pathway seemed to be slightly repressed under HL, which agrees with the observed increase in T6P levels under HL (Figs 2, 3, 6) and its known inhibitory effect on SnRK1 activity. SnRK1 extracted from source leaves is typically much less inhibited by T6P than that from sink tissues (Zhang *et al.*, 2009; Henry *et al.*, 2015). In this study, the *in vitro* SnRK1 activity was not directly affected by light intensity, but may have been modulated *in vivo* by changes in leaf T6P content, which correlated with its strong *in vitro* inhibition by T6P and the expression of well-characterized SnRK1 downstream targets (Figs 2, 3, 6), which clearly responded to light and associated changes in T6P. However, there was less good correlation when analyzing the overall set of SnRK1 target genes previously characterized in Arabidopsis (Fig. 6; Supplementary Table S2). This may indicate that different subsets of genes could respond to SnRK1 in tissue- and/or a C_4-dependent manner. Glucose usually activates TOR, which generally acts antagonistically to SnRK1, to promote growth by triggering the down- and up-regulation of hundreds of genes involved in catabolism and anabolism in sink tissues (Xiong *et al.*, 2013; Tomé *et al.*, 2014; Baena-González and Hanson, 2017). In this study, we did not observe a response of TOR to LL or HL, indicating that this pathway might not play a critical role in the response to light intensity and sugar levels in C_4 source leaves, at least not with our experimental system over the time frame we investigated (Fig. 6; Supplementary Table S2). Although the ectopic overexpression of *AtTOR* improved rice photosynthesis and water use efficiency, especially under water limitation (Bakshi *et al.*, 2017), most studies conducted on Arabidopsis showed that the TOR signalling pathway plays a critical role in young developing sink tissues rather than in source leaves (Anderson *et al.*, 2005; Deprost *et al.*, 2005, 2007;

Leiber *et al.*, 2010; Montané and Menand, 2013; Xiong *et al.*, 2013). This could explain why TOR was not activated by HL and glucose accumulation in the source leaves of *S. viridis*. In summary, the effects of light intensity and sugar levels on sugar signalling in C_4 source leaves differs from what has been previously reported for C_3 source leaves and sink tissues.

Several hypotheses may explain the unexpected sugar signalling responses we observed. The list of TOR and SnRK1 downstream targets used as references in our study were identified based on studies carried out on Arabidopsis or transgenic mesophyll protoplasts over- or underexpressing SnRK1 (Baena-González and Sheen, 2008; Xiong *et al.*, 2013). We used attached source C_4 monocot *S. viridis* leaves which differ from Arabidopsis C_3 dicots in their leaf anatomy and physiology (between mesophyll and bundle sheath cells) and light requirement. The set of SnRK1 downstream targets may differ between: (i) intact leaves and isolated protoplasts; (ii) C_3 and C_4 mesophyll cells; and (iii) bundle sheath and mesophyll cells in C_4 plants due to the contrasting partitioning of sucrose and starch biosynthesis in C_4 leaves (Lunn and Furbank, 1999).

The regulation of SnRK1 downstream targets in C_3 and C_4 species may also have different threshold sugar levels required to trigger sugar signalling responses. In C_4 maize sink tissue, for example, the SnRK1 K_i for inhibition by T6P was 50 μM (Nuccio *et al.*, 2015) compared with 4–5 μM in Arabidopsis seedlings (Nunes *et al.*, 2013). According to our results using C_4 source leaves and additional data mining of experiments using C_3 Arabidopsis shoots, leaves, or seedlings, the activation of the HXK-dependent pathway appears to require high sugar accumulation, irrespective of the species (Van Aken *et al.*, 2013; Xiong *et al.*, 2013; Y. Li *et al.*, 2015). On the other hand, the SnRK1 targets have been authenticated at physiological levels of sugar accumulation in response to low temperature and low nitrogen that induce sugar accumulation and in response to feeding sucrose at physiological levels (Zhang *et al.*, 2009; Nunes *et al.*, 2013). Genes regulated by glucose through the TOR pathway in Arabidopsis were identified after 2 h of treatment with only 15 mM glucose (Xiong *et al.*, 2013). Hence, the unexpected sugar signalling responses we observed may reflect a systematic difference in the threshold of sugar sensitivity between different sugar sensors and/or between C_3 and C_4 tissues, which will be the focus of our future research.

Alternatively, the response of *S. viridis* C_4 leaves to LL and HL, and the resulting changes in sugar levels, may have involved other sugar signalling pathways that have not yet been characterized in plants. Additionally, the response of C_4 source leaves to LL and HL may be predominantly triggered by light signalling pathways. Chloroplasts have been involved in plant responses to fluctuating light intensities through a process called 'retrograde signalling'. Chloroplast retrograde signalling can alter the expression of various genes, especially genes involved in photosynthesis (Szechyńska-Hebda and Karpiński, 2013; Chan *et al.*, 2016). Changes in light intensity are also sensed by phytochrome light sensors through a shift in the ratio of red to far red light, which usually occurs under shading (Jiao *et al.*, 2007; Bae and Choi, 2008; Van Buskirk *et al.*, 2012; Xu *et al.*, 2015). Since C_4 source leaves have very high light requirements and rely on it to produce sugars, in contrast to sink tissues, which rely on imported sugars to develop and grow, light signalling might over-ride sugar signalling in *S. viridis* leaves.

Sugar versus light signalling pathways in source leaves of C_4 S. viridis

Although our experimental design does not allow us to separate light- from sugar-related signalling responses, we attempted to interpret our results with data available in the literature. Consequently, we compared the effect of sugars and light on the expression of the downstream targets of HXK, TOR, and SnRK1, between our experiments and similar experiments using *Arabidopsis thaliana* (Van Aken *et al.*, 2013; Xiong *et al.*, 2013; Y. Li *et al.*, 2015). In *A. thaliana* plants treated with darkness or HL (1000 μmol m^{-2} s^{-1}), the expression of HXK downstream targets was affected, but not in a clear fashion. Most of the HXK-repressible targets were repressed under both darkness and HL. Additionally, those targets were not clearly affected by the addition of physiological levels of glucose (15 mM) or sucrose (1%) (Supplementary Table S4; Supplementary Fig. S7). Hence, in Arabidopsis, the expression of the key HXK downstream targets seems to be affected by darkness and HL, but not by low levels of sugars as reported in studies in which these genes were originally identified. The discrepancy in the literature may be due to the relatively high (2–3% of sucrose or 50–300 mM sucrose or glucose) level of sugars used to identify these genes (Jang and Sheen, 1994; Jang *et al.*, 1997; Zhou *et al.*, 1998; Sheen *et al.*, 1999; Xiao *et al.*, 2000; Moore *et al.*, 2003; Kunz *et al.*, 2014, 2015). Taken together, these results indicate that HXK might be more responsive to light intensity than to physiologically relevant changes in glucose levels and that the HXK-dependent pathway might require dramatic changes in glucose levels to be activated in both C_3 and C_4 species. Hence, the unexpected induction of the HXK-dependent pathway we observed under LL and sugar depletion is likely to be due to the effect of light rather than sugars. Similarly, the absence of the expected activation of the HXK-dependent pathway by HL and sugar accumulation in *S. viridis*, in contrast to initial reports using Arabidopsis fed with high sugar levels, is consistent with our re-analysis of the published data sets using low sugar concentrations. These results indicate that the absence of the activation of the HXK-dependent pathway we observed under HL is probably due to an insufficient change in sugar levels and/or the over-riding effect of light signalling.

On the other hand, in re-analysed data, the expression of the key downstream targets of TOR and SnRK1 in Arabidopsis is more clearly and consistently affected by sugars, although they can also be regulated by light (Supplementary Table S4; Supplementary Fig. S7). These results indicate that in our experiments, the SnRK1 signalling pathway is more likely to be activated by sugar depletion under LL and repressed by sugar accumulation under HL than by the light intensity itself. We are currently using sugar sensing mutants to further investigate this hypothesis. Finally, TOR was not affected by changes in sugar levels or light intensity in our study, unlike observations using similar experiments in Arabidopsis, which indicates possible differences between species and/or source and sink tissues.

Supplementary data

Supplementary data are available at *JXB* online.

Table S1. A_{net}/C_i, fluorescence, and chlorophyll content parameters in light-treated *S. viridis* leaves.

Table S2. Number of key transcripts affected by light treatments in *S. viridis* leaves.

Table S3. Mapman4 gene category enrichment in light-treated *S. viridis* leaves.

Table S4. Summary of the effect of darkness, high light, glucose, and sucrose on the transcript levels of key sugar signalling targets in *A. thaliana*.

Table S5. Log2 FC and classification of all DE transcripts in light-treated *S. viridis* leaves.

Table S6. List of *S. italica* photosynthesis gene transcripts used to analyse the RNAseq data.

Table S7. List of *S. italica* sugar signalling and trehalose pathway genes used to analyse the RNAseq data.

Table S8. List of *S. italica* key HXK downstream target genes transcripts used to analyse the RNAseq data.

Table S9. List of *S. italica* key TOR downstream target genes transcripts used to analyse the RNAseq data.

Table S10. List of *S. italica* key SnRK1 downstream target genes transcripts used to analyse the RNAseq data.

Table S11. List of *S. italica* all putative TOR downstream target genes transcripts used to analyse the RNAseq data.

Table S12. List of *S. italica* all putative SnRK1 downstream target genes transcripts used to analyse the RNAseq data.

Fig. S1. Experimental design and phenotype of *S. viridis* plants after light treatments.

Fig. S2. Time for light-treated *S. viridis* leaves to reach steady state at high irradiance.

Fig. S3. A_{net}/C_i curves of light-treated *S. viridis* leaves at high irradiance.

Fig. S4. *In vitro* activity and content of key photosynthetic enzymes from light-treated *S. viridis* leaves.

Fig. S5. Relative level of fructose, sucrose-6-phophate, and trehalose in light-treated *S. viridis* leaves.

Fig. S6. Dynamic changes of the whole transcriptome and the full sets of TOR and SnRK1 predicted downstream targets in light-treated *S. viridis* leaves.

Fig. S7. Effect of darkness, high light, glucose, and sucrose on the transcript levels of our key sugar signalling targets in *A. thaliana*.

Protocol S1. Detailed protocol used to extract and measure the activity of PEPC, NADP-ME, and Rubisco activity, adapted from Sharwood *et al*. (2016*b*).

Protocol S2. Detailed protocol used to perform SDS–PAGE and western blots against PEPC, NADP-ME, and Rubisco using a method as in Sharwood *et al*. (2014).

Protocol S3. Methods for determination of the list of *S. italica* transcripts used to identify photosynthetic genes, sugar sensors, trehalose pathway genes, and putative sugar signalling targets (including Supplementary Tables S6–S12).

Acknowledgements

We thank Fiona Koller, Bethanie Coleman, and Samantha Prior for their technical assistance. This research was funded by the ARC Centre of Excellence for Translational Photosynthesis (CE140100015) awarded to OG and RTF. Rothamsted Research receives strategic funding from the Biotechnological and Biological Sciences Research Council of the United Kingdom. We acknowledge support through the designing future wheat (DFW) strategic programme (BB/P016855/1).

References

Anderson GH, Veit B, Hanson MR. 2005. The Arabidopsis AtRaptor genes are essential for post-embryonic plant growth. BMC Biology **3**, 12.

Andrès C, Agne B, Kessler F. 2010. The TOC complex: preprotein gateway to the chloroplast. Biochimica et Biophysica Acta **1803**, 715–723.

Bae G, Choi G. 2008. Decoding of light signals by plant phytochromes and their interacting proteins. Annual Review of Plant Biology **59**, 281–311.

Baena-González E. 2010. Energy signaling in the regulation of gene expression during stress. Molecular Plant **3**, 300–313.

Baena-González E, Hanson J. 2017. Shaping plant development through the SnRK1–TOR metabolic regulators. Current Opinion in Plant Biology **35**, 152–157.

Baena-González E, Rolland F, Thevelein JM, Sheen J. 2007. A central integrator of transcription networks in plant stress and energy signalling. Nature **448**, 938–942.

Baena-González E, Sheen J. 2008. Convergent energy and stress signaling. Trends in Plant Science **13**, 474–482.

Bakshi A, Moin M, Kumar MU, Reddy AB, Ren M, Datla R, Siddiq EA, Kirti PB. 2017. Ectopic expression of *Arabidopsis Target of Rapamycin* (*AtTOR*) improves water-use efficiency and yield potential in rice. Scientific Reports **7**, 42835.

Bennetzen JL, Schmutz J, Wang H, *et al*. 2012. Reference genome sequence of the model plant *Setaria*. Nature Biotechnology **30**, 555–561.

Bläsing OE, Gibon Y, Günther M, Höhne M, Morcuende R, Osuna D, Thimm O, Usadel B, Scheible WR, Stitt M. 2005. Sugars and circadian regulation make major contributions to the global regulation of diurnal gene expression in Arabidopsis. The Plant Cell **17**, 3257–3281.

Bolger AM, Lohse M, Usadel B. 2014. Trimmomatic: a flexible trimmer for Illumina sequence data. Bioinformatics **30**, 2114–2120.

Bracher A, Whitney SM, Hartl FU, Hayer-Hartl M. 2017. Biogenesis and metabolic maintenance of Rubisco. Annual Review of Plant Biology **68**, 29–60.

Brauner K, Stutz S, Paul M, Heyer AG. 2015. Measuring whole plant CO_2 exchange with the environment reveals opposing effects of the gin2-1 mutation in shoots and roots of *Arabidopsis thaliana*. Plant Signaling & Behavior **10**, e973822.

Browning KS, Bailey-Serres J. 2015. Mechanism of cytoplasmic mRNA translation. The Arabidopsis Book **13**, e0176.

Brutnell TP, Wang L, Swartwood K, Goldschmidt A, Jackson D, Zhu XG, Kellogg E, Van Eck J. 2010. *Setaria viridis*: a model for C4 photosynthesis. The Plant Cell **22**, 2537–2544.

Caldana C, Li Y, Leisse A, Zhang Y, Bartholomaeus L, Fernie AR, Willmitzer L, Giavalisco P. 2013. Systemic analysis of inducible target of rapamycin mutants reveal a general metabolic switch controlling growth in *Arabidopsis thaliana*. The Plant Journal **73**, 897–909.

Chan KX, Phua SY, Crisp P, McQuinn R, Pogson BJ. 2016. Learning the languages of the chloroplast: retrograde signaling and beyond. Annual Review of Plant Biology **67**, 25–53.

Cho JI, Ryoo N, Eom JS, *et al*. 2008. Role of the rice hexokinases OsHXK5 and OsHXK6 as glucose sensors. Plant Physiology **149**, 745–759.

Cho YH, Hong JW, Kim EC, Yoo SD. 2012. Regulatory functions of SnRK1 in stress-responsive gene expression and in plant growth and development. Plant Physiology **158**, 1955–1964.

Dai N, Schaffer A, Petreikov M, Shahak Y, Giller Y, Ratner K, Levine A, Granot D. 1999. Overexpression of Arabidopsis hexokinase in tomato plants inhibits growth, reduces photosynthesis, and induces rapid senescence. The Plant Cell **11**, 1253–1266.

Deprost D, Truong HN, Robaglia C, Meyer C. 2005. An Arabidopsis homolog of RAPTOR/KOG1 is essential for early embryo development. Biochemical and Biophysical Research Communications **326**, 844–850.

Deprost D, Yao L, Sormani R, Moreau M, Leterreux G, Nicolaï M, Bedu M, Robaglia C, Meyer C. 2007. The Arabidopsis TOR kinase links plant growth, yield, stress resistance and mRNA translation. EMBO Reports **8**, 864–870.

Ding Z, Zhang Y, Xiao Y, *et al*. 2016. Transcriptome response of cassava leaves under natural shade. Scientific Reports **6**, 31673.

Dobrenel T, Marchive C, Sormani R, Moreau M, Mozzo M, Montané MH, Menand B, Robaglia C, Meyer C. 2011. Regulation of plant growth and metabolism by the TOR kinase. Biochemical Society Transactions **39**, 477–481.

Dong P, Xiong F, Que Y, Wang K, Yu L, Li Z, Ren M. 2015. Expression profiling and functional analysis reveals that TOR is a key player in regulating photosynthesis and phytohormone signaling pathways in Arabidopsis. Frontiers in Plant Science **6**, 677.

Figueroa CM, Lunn JE. 2016. A tale of two sugars: trehalose 6-phosphate and sucrose. Plant Physiology **172**, 7–27.

Flores-Pérez Ú, Jarvis P. 2013. Molecular chaperone involvement in chloroplast protein import. Biochimica et Biophysica Acta **1833**, 332–340.

Ghannoum O, Evans JR, von Caemmerer S. 2011. Nitrogen and water use efficiency of C_4 plants. In: Raghavendra AS, Sage RF, eds. C_4 photosynthesis and related CO_2 concentrating mechanisms. Dordrecht, The Netherlands: Springer, 129–146.

Goldschmidt EE, Huber SC. 1992. Regulation of photosynthesis by end-product accumulation in leaves of plants storing starch, sucrose, and hexose sugars. Plant Physiology **99**, 1443–1448.

Gong W, Qi P, Du J, *et al*. 2014. Transcriptome analysis of shade-induced inhibition on leaf size in relay intercropped soybean. PLoS One **9**, e98465.

Griffiths CA, Paul MJ, Foyer CH. 2016. Metabolite transport and associated sugar signalling systems underpinning source/sink interactions. Biochimica et Biophysica Acta **1857**, 1715–1725.

Hatch MD. 1987. C4 photosynthesis: a unique blend of modified biochemistry, anatomy and ultrastructure. Biochimica et Biophysica Acta **895**, 81–106.

Henriques R, Bögre L, Horváth B, Magyar Z. 2014. Balancing act: matching growth with environment by the TOR signalling pathway. Journal of Experimental Botany **65**, 2691–2701.

Henry C, Bledsoe SW, Griffiths CA, Kollman A, Paul MJ, Sakr S, Lagrimini LM. 2015. Differential role for trehalose metabolism in salt-stressed maize. Plant Physiology **169**, 1072–1089.

Jang JC, León P, Zhou L, Sheen J. 1997. Hexokinase as a sugar sensor in higher plants. The Plant Cell **9**, 5–19.

Jang JC, Sheen J. 1994. Sugar sensing in higher plants. The Plant Cell **6**, 1665–1679.

Jiao Y, Lau OS, Deng XW. 2007. Light-regulated transcriptional networks in higher plants. Nature Reviews. Genetics **8**, 217–230.

John CR, Smith-Unna RD, Woodfield H, Covshoff S, Hibberd JM. 2014. Evolutionary convergence of cell-specific gene expression in independent lineages of C4 grasses. Plant Physiology **165**, 62–75.

Kalt-Torres W, Kerr PS, Usuda H, Huber SC. 1987. Diurnal changes in maize leaf photosynthesis: I. Carbon exchange rate, assimilate export rate, and enzyme activities. Plant Physiology **83**, 283–288.

Karki S, Rizal G, Quick WP. 2013. Improvement of photosynthesis in rice (*Oryza sativa* L.) by inserting the C4 pathway. Rice **6**, 28.

Kelly G, David-Schwartz R, Sade N, Moshelion M, Levi A, Alchanatis V, Granot D. 2012. The pitfalls of transgenic selection and new roles of *AtHXK1*: a high level of *AtHXK1* expression uncouples hexokinase1-dependent sugar signaling from exogenous sugar. Plant Physiology **159**, 47–51.

Kelly G, Moshelion M, David-Schwartz R, Halperin O, Wallach R, Attia Z, Belausov E, Granot D. 2013. Hexokinase mediates stomatal closure. The Plant Journal **75**, 977–988.

Kelly G, Sade N, Attia Z, Secchi F, Zwieniecki M, Holbrook NM, Levi A, Alchanatis V, Moshelion M, Granot D. 2014. Relationship between hexokinase and the aquaporin PIP1 in the regulation of photosynthesis and plant growth. PLoS One **9**, e87888.

Kikuchi S, Bédard J, Hirano M, Hirabayashi Y, Oishi M, Imai M, Takase M, Ide T, Nakai M. 2013. Uncovering the protein translocon at the chloroplast inner envelope membrane. Science **339**, 571–574.

Krapp A, Stitt M. 1995. An evaluation of direct and indirect mechanisms for the 'sink-regulation' of photosynthesis in spinach: changes in gas exchange, carbohydrates, metabolites, enzyme activities and steady-state transcript levels after cold-girdling source leaves. Planta **195**, 313–323.

Kretzschmar T, Pelayo MA, Trijatmiko KR, *et al*. 2015. A trehalose-6-phosphate phosphatase enhances anaerobic germination tolerance in rice. Nature Plants **1**, 15124.

Krishna P, Gloor G. 2001. The Hsp90 family of proteins in *Arabidopsis thaliana*. Cell Stress & Chaperones **6**, 238–246.

Kunz S, Gardeström P, Pesquet E, Kleczkowski LA. 2015. Hexokinase 1 is required for glucose-induced repression of bZIP63, At5g22920, and BT2 in Arabidopsis. Frontiers in Plant Science **6**, 525.

Kunz S, Pesquet E, Kleczkowski LA. 2014. Functional dissection of sugar signals affecting gene expression in *Arabidopsis thaliana*. PLoS One **9**, e100312.

Langmead B, Salzberg SL. 2012. Fast gapped-read alignment with Bowtie 2. Nature Methods **9**, 357–359.

Leegood RC. 2000. Transport during C4 photosynthesis. In: Leegood RC, Sharkey TD, von Caemmerer S, eds. Photosynthesis. Advances in Photosynthesis and Respiration. Dordrecht, The Netherlands: Springer, 459–469.

Leiber RM, John F, Verhertbruggen Y, Diet A, Knox JP, Ringli C. 2010. The TOR pathway modulates the structure of cell walls in Arabidopsis. The Plant Cell **22**, 1898–1908.

Li L, Sheen J. 2016. Dynamic and diverse sugar signaling. Current Opinion in Plant Biology **33**, 116–125.

Li L, Song Y, Wang K, Dong P, Zhang X, Li F, Li Z, Ren M. 2015. TOR-inhibitor insensitive-1 (TRIN1) regulates cotyledons greening in Arabidopsis. Frontiers in Plant Science **6**, 861.

Li P, Brutnell TP. 2011. *Setaria viridis* and *Setaria italica*, model genetic systems for the Panicoid grasses. Journal of Experimental Botany **62**, 3031–3037.

Li Y, Andrade J. 2017. DEApp: an interactive web interface for differential expression analysis of next generation sequence data. Source Code for Biology and Medicine **12**, 2.

Li Y, Mukherjee I, Thum KE, Tanurdzic M, Katari MS, Obertello M, Edwards MB, McCombie WR, Martienssen RA, Coruzzi GM. 2015. The histone methyltransferase SDG8 mediates the epigenetic modification of light and carbon responsive genes in plants. Genome Biology **16**, 79.

Lohse M, Nagel A, Herter T, May P, Schroda M, Zrenner R, Tohge T, Fernie AR, Stitt M, Usadel B. 2014. Mercator: a fast and simple web server for genome scale functional annotation of plant sequence data. Plant, Cell & Environment **37**, 1250–1258.

Love MI, Huber W, Anders S. 2014. Moderated estimation of fold change and dispersion for RNA-seq data with DESeq2. Genome Biology **15**, 550.

Lunn JE, Furbank RT. 1997. Localisation of sucrose-phosphate synthase and starch in leaves of C4 plants. Planta **202**, 106–111.

Lunn JE, Furbank RT. 1999. Sucrose biosynthesis in C_4 plants. New Phytologist **143**, 221–237.

Martínez-Barajas E, Delatte T, Schluepmann H, de Jong GJ, Somsen GW, Nunes C, Primavesi LF, Coello P, Mitchell RA, Paul MJ. 2011. Wheat grain development is characterized by remarkable trehalose 6-phosphate accumulation pregrain filling: tissue distribution and relationship to SNF1-related protein kinase1 activity. Plant Physiology **156**, 373–381.

Merchante C, Stepanova AN, Alonso JM. 2017. Translation regulation in plants: an interesting past, an exciting present and a promising future. The Plant Journal **90**, 628–653.

Montané MH, Menand B. 2013. ATP-competitive mTOR kinase inhibitors delay plant growth by triggering early differentiation of meristematic cells but no developmental patterning change. Journal of Experimental Botany **64**, 4361–4374.

Moore B, Zhou L, Rolland F, Hall Q, Cheng WH, Liu YX, Hwang I, Jones T, Sheen J. 2003. Role of the Arabidopsis glucose sensor HXK1 in nutrient, light, and hormonal signaling. Science **300**, 332–336.

Nakai M. 2015. The TIC complex uncovered: the alternative view on the molecular mechanism of protein translocation across the inner envelope membrane of chloroplasts. Biochimica et Biophysica Acta **1847**, 957–967.

Nishimura K, Ogawa T, Ashida H, Yokota A. 2008. Molecular mechanisms of RuBisCO biosynthesis in higher plants. Plant Biotechnology **25**, 285–290.

Nuccio ML, Wu J, Mowers R, *et al*. 2015. Expression of trehalose-6-phosphate phosphatase in maize ears improves yield in well-watered and drought conditions. Nature Biotechnology **33**, 862–869.

Nukarinen E, Nägele T, Pedrotti L, *et al*. 2016. Quantitative phosphoproteomics reveals the role of the AMPK plant ortholog SnRK1 as a metabolic master regulator under energy deprivation. Scientific Reports **6**, 31697.

Nunes C, O'Hara LE, Primavesi LF, Delatte TL, Schluepmann H, Somsen GW, Silva AB, Fevereiro PS, Wingler A, Paul MJ. 2013. The trehalose 6-phosphate/SnRK1 signaling pathway primes growth recovery following relief of sink limitation. Plant Physiology **162**, 1720–1732.

Oszvald M, Primavesi LF, Griffiths CA, Cohn J, Basu SS, Nuccio ML, Paul MJ. 2018. Trehalose 6-phosphate regulates photosynthesis and assimilate partitioning in reproductive tissue. Plant Physiology **176**, 2623–2638.

Pant SR, Irigoyen S, Doust AN, Scholthof KB, Mandadi KK. 2016. *Setaria*: a food crop and translational research model for C4 grasses. Frontiers in Plant Science **7**, 1885.

Paul MJ, Foyer CH. 2001. Sink regulation of photosynthesis. Journal of Experimental Botany **52**, 1383–1400.

Paul MJ, Pellny TK. 2003. Carbon metabolite feedback regulation of leaf photosynthesis and development. Journal of Experimental Botany **54**, 539–547.

Pellny TK, Ghannoum O, Conroy JP, Schluepmann H, Smeekens S, Andralojc J, Krause KP, Goddijn O, Paul MJ. 2004. Genetic modification of photosynthesis with *E. coli* genes for trehalose synthesis. Plant Biotechnology Journal **2**, 71–82.

Porra RJ, Thompson WA, Kriedemann PE. 1989. Determination of accurate extinction coefficients and simultaneous equations for assaying chlorophylls a and b extracted with four different solvents: verification of the concentration of chlorophyll standards by atomic absorption spectroscopy. Biochimica et Biophysica Acta **975**, 384–394.

Ramon M, Rolland F. 2007. Plant development: introducing trehalose metabolism. Trends in Plant Science **12**, 185–188.

R Core Team. 2016. R: a language and environment for statistical computing. Vienna, Austria: R Foundation for Statistical Computing.

Rexin D, Meyer C, Robaglia C, Veit B. 2015. TOR signalling in plants. The Biochemical Journal **470**, 1–14.

Roberts A, Pachter L. 2013. Streaming fragment assignment for real-time analysis of sequencing experiments. Nature Methods **10**, 71–73.

Rolland F, Baena-Gonzalez E, Sheen J. 2006. Sugar sensing and signaling in plants: conserved and novel mechanisms. Annual Review of Plant Biology **57**, 675–709.

RStudio Team. 2015. RStudio: integrated development for R. Boston, MA: RStudio, Inc. http://www.rstudio.com/.

Sage RF, Pearcy RW. 2000. The physiological ecology of C4 photosynthesis. Dordrecht, The Netherlands: Springer, 497–532.

Sage RF, Sage TL, Kocacinar F. 2012. Photorespiration and the evolution of C4 photosynthesis.

Sebastian J, Wong MK, Tang E, Dinneny JR. 2014. Methods to promote germination of dormant *Setaria viridis* seeds. PLoS One **9**, e95109.

Sharwood RE, Ghannoum O, Whitney SM. 2016*a*. Prospects for improving CO2 fixation in C3-crops through understanding C4-Rubisco biogenesis and catalytic diversity. Current Opinion in Plant Biology **31**, 135–142.

Sharwood RE, Sonawane BV, Ghannoum O. 2014. Photosynthetic flexibility in maize exposed to salinity and shade. Journal of Experimental Botany **65**, 3715–3724.

Sharwood RE, Sonawane BV, Ghannoum O, Whitney SM. 2016*b*. Improved analysis of C_4 and C_3 photosynthesis via refined *in vitro* assays of their carbon fixation biochemistry. Journal of Experimental Botany **67**, 3137–3148.

Sheen J. 1990. Metabolic repression of transcription in higher plants. The Plant Cell **2**, 1027–1038.

Sheen J, Zhou L, Jang JC. 1999. Sugars as signaling molecules. Current Opinion in Plant Biology **2**, 410–418.

Sung DY, Vierling E, Guy CL. 2001. Comprehensive expression profile analysis of the Arabidopsis Hsp70 gene family. Plant Physiology **126**, 789–800.

Szechyńska-Hebda M, Karpiński S. 2013. Light intensity-dependent retrograde signalling in higher plants. Journal of Plant Physiology **170**, 1501–1516.

Thimm O, Bläsing O, Gibon Y, Nagel A, Meyer S, Krüger P, Selbig J, Müller LA, Rhee SY, Stitt M. 2004. MAPMAN: a user-driven tool to display genomics data sets onto diagrams of metabolic pathways and other biological processes. The Plant Journal **37**, 914–939.

Tomé F, Nägele T, Adamo M, *et al*. 2014. The low energy signaling network. Frontiers in Plant Science **5**, 353.

Trösch R, Mühlhaus T, Schroda M, Willmund F. 2015. ATP-dependent molecular chaperones in plastids—more complex than expected. Biochimica et Biophysica Acta **1847**, 872–888.

Usuda H, Edwards GE. 1984. Is photosynthesis during the induction period in maize limited by the availability of intercellular carbon dioxide? Plant Science Letters **37**, 41–45.

Usuda H, Kalt-Torres W, Kerr PS, Huber SC. 1987. Diurnal changes in maize leaf photosynthesis: II. Levels of metabolic intermediates of sucrose synthesis and the regulatory metabolite fructose 2,6-bisphosphate. Plant Physiology **83**, 289–293.

Usuda H, Ku MSB, Edwards GE. 1985. Influence of light intensity during growth on photosynthesis and activity of several key photosynthetic enzymes in a C_4 plant (*Zea mays*). Physiologia Plantarum **63**, 65–70.

Van Aken O, Zhang B, Law S, Narsai R, Whelan J. 2013. AtWRKY40 and AtWRKY63 modulate the expression of stress-responsive nuclear genes encoding mitochondrial and chloroplast proteins. Plant Physiology **162**, 254–271.

Van Buskirk EK, Decker PV, Chen M. 2012. Photobodies in light signaling. Plant Physiology **158**, 52–60.

Wang P, Vlad D, Langdale JA. 2016. Finding the genes to build C4 rice. Current Opinion in Plant Biology **31**, 44–50.

Watson-Lazowski A, Papanicolaou A, Sharwood R, Ghannoum O. 2018. Investigating the NAD-ME biochemical pathway within C4 grasses using transcript and amino acid variation in C4 photosynthetic genes. Photosynthesis Research **138**, 233–248.

Xiao W, Sheen J, Jang JC. 2000. The role of hexokinase in plant sugar signal transduction and growth and development. Plant Molecular Biology **44**, 451–461.

Xiong F, Zhang R, Meng Z, Deng K, Que Y, Zhuo F, Feng L, Guo S, Datla R, Ren M. 2017. Brassinosteriod insensitive 2 (BIN2) acts as a downstream effector of the target of rapamycin (TOR) signaling pathway to regulate photoautotrophic growth in Arabidopsis. New Phytologist **213**, 233–249.

Xiong Y, McCormack M, Li L, Hall Q, Xiang C, Sheen J. 2013. Glucose–TOR signalling reprograms the transcriptome and activates meristems. Nature **496**, 181–186.

Xiong Y, Sheen J. 2015. Novel links in the plant TOR kinase signaling network. Current Pinion in Plant Biology **28**, 83–91.

Xu X, Paik I, Zhu L, Huq E. 2015. Illuminating progress in phytochrome-mediated light signaling pathways. Trends in Plant Science **20**, 641–650.

Zhang Y, Primavesi LF, Jhurreea D, Andralojc PJ, Mitchell RA, Powers SJ, Schluepmann H, Delatte T, Wingler A, Paul MJ. 2009. Inhibition of SNF1-related protein kinase1 activity and regulation of metabolic pathways by trehalose-6-phosphate. Plant Physiology **149**, 1860–1871.

Zhou L, Jang JC, Jones TL, Sheen J. 1998. Glucose and ethylene signal transduction crosstalk revealed by an Arabidopsis glucose-insensitive mutant. Proceedings of the National Academy of Sciences, USA **95**, 10294–10299.